RSC Advances

PAPER

View Article Online
View Journal | View Issue

Cite this: *RSC Adv.*, 2026, **16**, 14630

Synthesis of lignin nanoparticles using CO_2-responsive amines and their performance as UV-light shields

Olga Torres-Rocha,[ab] Maedeh Ramezani,[ab] Michael Cunningham *[ab] and Philip G. Jessop *[a]

Received 19th February 2026
Accepted 9th March 2026

DOI: 10.1039/d6ra01472k

rsc.li/rsc-advances

Lignin is biosourced, abundant, biodegradable and renewable, and therefore an appealing feedstock from which to make materials for applications in diverse fields. In this work, we report the initial results of a new method to produce lignin nanoparticles (LNP) with tailored particle size. Lignin is first dispersed at elevated pH in an aqueous solution of a CO_2-responsive amine, after which the addition of CO_2 at atmospheric pressure induces precipitation of the lignin as nanoparticles. Two different CO_2-responsive amines, TMBDA (*N*,*N*,*N*′,*N*′-tetramethyl-1,4-butanediamine) and TMTAD (2,6,10-trimethyl-2,6,10-triazaundecane), were evaluated for their effect on the lignin particle size and yield. For both amines, particle sizes were in the range of 125–175 nm with narrow particle size distributions. Yields were >84% for TMBDA and >94% for TMTAD. These LNP, when dispersed in poly(vinyl alcohol) (PVA) films, provide promising UV blockage even at low LNP content.

Introduction

As the demand to replace petroleum-based polymeric materials and find more sustainably-sourced alternatives increases, interest in the development of new bio-based materials has increased dramatically. A promising option is lignin, a readily available and inexpensive bio-based feedstock found in the lignocellulose of plants and wood. Lignocellulose is composed of lignin, cellulose and hemicellulose, with approximate compositions of 15–30 wt%, 30–50 wt% and 20–35 wt% respectively.[1–3] In the pulp and paper industry, lignocellulose is treated to obtain cellulose, while hemicellulose and lignin are discarded as waste products. However, lignin possesses several desirable properties. It is biocompatible, biodegradable, renewable, non-toxic and chemically and biologically resistant, and exhibits oxidative and UV resistance as well as antibacterial properties.[1–6] Lignin, with an amorphous polymeric structure and different functional groups,[11] is readily amenable to chemical modification or polymer grafting to provide numerous new properties for targeted applications.[1,6] Unlike many other biopolymers, lignin itself can exhibit good mechanical and physical properties as films, fibers, nanoparticles (LNP), or other morphologies.[6]

There are different processes used to remove lignin from lignocellulose such as the Kraft, sulfite, soda processes, or organic solvent extraction. The Kraft process, which is the most commonly used, employs alkaline conditions (pH ∼ 13–14) with strong base such as sodium hydroxide or sodium sulfide at high temperatures (∼170 °C). Then, after the alkaline treatment, lignin is precipitated from the alkaline solution by a washing process using acids such as sulfuric acid to lower the pH to ∼5–7.5. In the sulfite process, another method to obtain lignin from lignocellulose, sulfur dioxide and metal (Na^{2+}, Ca^{2+}, Mg^{2+}) sulfites are used at 120–180 °C. The soda process employs sodium hydroxide and anthraquinone at 140–170 °C. Finally, a less common process involves a mixture of water with either methanol, ethanol, acetic or formic acid used at high temperatures (∼190 °C).6–9

Lignin is comprised primarily of phenylpropanolic monomers such as sinapyl alcohol, *p*-coumaryl alcohol, and coniferyl alcohol, as well as ketones.[1,5,6] Although these monomers have been identified, lignin is a complex and largely non-repeating polymer, the structure and molecular weight of which may vary according to the extraction process and source that is used to obtain it.[1,6,10]

Lignin nanoparticles (LNP) have attracted interest because their morphological structure can be tailored, maintaining the main properties of lignin while possessing very high surface area, high surface reactivity and potentially enhancing dispersion/dispersion capabilities in different environments.[12,13] The primary methods to prepare LNP reported in the literature include solvent exchange, pH-shifting, aerosol evaporation, supercritical fluid processing, and polymerization.[1,3,4,6,10–15] Each method can potentially yield LNP with a range of particle sizes, narrow or broad size distribution,

[a]*Department of Chemistry, Queen's University. 90 Bader Lane, Kingston, Ontario K7L 3N6, Canada. E-mail: jessop@queensu.ca; Michael.Cunningham@queensu.ca*
[b]*Department of Chemical Engineering, Queen's University, 19 Division St., Kingston, Ontario K7L 3N6, Canada*

and different shapes and morphologies (*e.g.* hollow, solid, tube-shaped or fibers). For approaches using solvent exchange/anti-solvent precipitation, pH-shifting, and aerosol evaporation, the lignin needs to be solubilized. For the aerosol process, the lignin solution is atomized to small droplets before being dried, producing LNP ~100 nm.[16] In the pH-shifting process, the lignin solution is precipitated in acid media,[17–19] with the size of the LNP being determined by the acid concentration and the source of lignin.[17–19] In the solvent exchange process, a lignin solution (*e.g.* 1,4-dioxane) is added to a non-solvent (*e.g.* water or cyclohexane). Once the LNP are formed, the solvent is evaporated to yield a nanoparticle dispersion. The choice of the solvent/anti-solvent system plays a critical role in the success of the process. The particle size can vary from ~50 to ~250 nm, with both narrow and broad particle size distributions potentially produced.[20,21] Supercritical (sc) fluids such as $scCO_2$ have also been used for the preparation of LNP. In this case, lignin is solubilized in an organic solvent such as acetone or *N*,*N*-dimethylformamide (DMF) and then precipitated in $scCO_2$ to yield LNP. Particle sizes in the range of 38–280 nm have reported.[22,23] Polymer grafting has also been employed to obtain LNP. The grafted polymer largely determines the final properties of the resulting LNP. For example, poly(2-(diethyl-amino) ethyl methacrylate) (PDEAEMA) has been grafted to lignin, with the resulting particles exhibiting CO_2/N_2-switchability for reversible dispersion/precipitation.[14] The chosen method should ideally be simple and inexpensive with high yields. Narrow particle size distributions are often also desirable.

The preparation of LNP *via* acid precipitation (or precipitation in acids as antisolvents) is a popular method, yielding LNP from ~84 to 450 nm with spherical/semi-spherical morphologies. Common solvents used to solubilize the LNP are ethylene glycol, sodium hydroxide solutions, or mixtures of water and ethanol, while the acids used to precipitate the LNP include hydrochloric acid, sulfuric acid or nitric acid.[24–29] Systems involving organic solvents such as DMF and CO_2 at high pressure have also been used to prepare LNP with a size of 38 nm.[30] Although these are successful methods to prepare LNP and present numerous advantages, there are still some challenges that need to be addressed such as avoiding or minimizing the use of harmful chemicals to make the process greener.

In this report, we present the proof of concept of a novel and simple method to obtain LNP using switchable water (SW).[31,32] SW is a stimuli-responsive aqueous solution that reversibly switches its properties upon the application or removal of a trigger, in our case CO_2. In the first step, Kraft lignin was brought to alkaline conditions (pH > 9.0) using aqueous solutions of *N*,*N*,*N*′,*N*′-tetramethyl-1,4-butanediamine (TMBDA) or 2,6,10-trimethyl-2,6,10-triazaundecane (TMTAD) under agitation. At this stage, the lignin is well-dispersed in the media. Solutions of TMBDA or TMTAD in water are examples of SW. Addition of CO_2 converts the amines to the corresponding bicarbonate salt, which causes many properties of the solution to change, notably ionic strength and the solubility of solutes in SW.[31,32] In our system, from the initial pH of >9.0, CO_2 at atmospheric pressure decreases the pH and induces precipitation of the LNP. The performance of TMTAD and TMBDA in obtaining LNP was evaluated. Average particle size (PS) was measured by dynamic light scattering (DLS), and morphology was confirmed *via* transmission electron microscopy (TEM).

Once the synthesis of LNP was confirmed, we also prepared PVA (poly(vinyl alcohol)) films loaded with different amounts of LNP and evaluated their capacity to act as UV light shields *via* UV-vis spectroscopy. The chemical functionalities present in lignin are capable of absorbing UV light, thereby providing UV-resistance to a polymer matrix if the LNP can be adequately dispersed in the polymer.[33–38] PVA-LNP films were prepared by a solvent casting process at different LNP loadings (2, 4 and 8 wt%) and compared against a control (LNP 0 wt%). PVA-LNP films were also analyzed *via* infrared spectroscopy (FTIR) to confirm their structure. The use of CO_2 as trigger to induce the precipitation of LNP is an attractive option as it is inexpensive, non-toxic, benign to the environment, and easily removed from the system, allowing recovery and re-use of the initial solution. Further, CO_2 switchable amines can be recycled and reused. The CO_2 gas used is an industrial waste product that is recycled in this process, which means that is not generated by this process, rather we are valorizing a waste that has already been produced.

Experimental

Materials

Lignin (Kraft lignin from softwood, West Fraser Mills Ltd), *N*,*N*,*N*′,*N*′-tetramethyl-1,4-butanediamine (TMBDA, TCI Chemicals, >98%) and 2,6,10-trimethyl-2,6,10-triazaundecane (TMTAD, TCI Chemicals, >96%) were used as received. Poly(-vinyl alcohol) (PVA) was obtained from Sigma-Aldrich (M_w 146 000–186 000, 87–89% hydrolyzed) and used as received.

Characterization methods

Particle size was measured by DLS (Dynamic Light Scattering) with a Malvern Zetasizer Nano ZS (size range 0.3 nm −10 μm) at 25 °C with non-invasive backscatter optics (173°), using a 4 mW He–Ne (633 nm) laser. All samples were measured in quartz cuvettes. Data was processed using the Malvern Dispersion Technology Software (v. 5.00). pH was measured using a benchtop pH meter (Seven Excellence from Mettler Toledo). Transmission electron microscopy (TEM) images were obtained in a Thermo Fisher Talos F200i S/TEM unit. FT-IR spectra were obtained using a Bruker Alpha FT-IR base spectrometer equipped with an ATR accessory. The transmittance of PVA-LNP films was measured with a UV-vis spectrometer (Thermo-Scientific spectrometer) from 200–800 nm using air as the background.

Synthesis of LNPs

In a typical procedure, first a SW solution was prepared by dissolving specific amounts of TMBDA (100 μL, 0.0792 g, 0.55 mmol) or TMTAD (100 μL, 0.083 g, 0.41 mmol) in 10 g of deionized (DI) water. After 60 min, lignin (0.21 g) was added to the TMTAD or TMBDA solution. The pH of the dispersion was measured right before CO_2 addition started. CO_2 was then purged for 30 min into the solution, using a gas dispersion tube

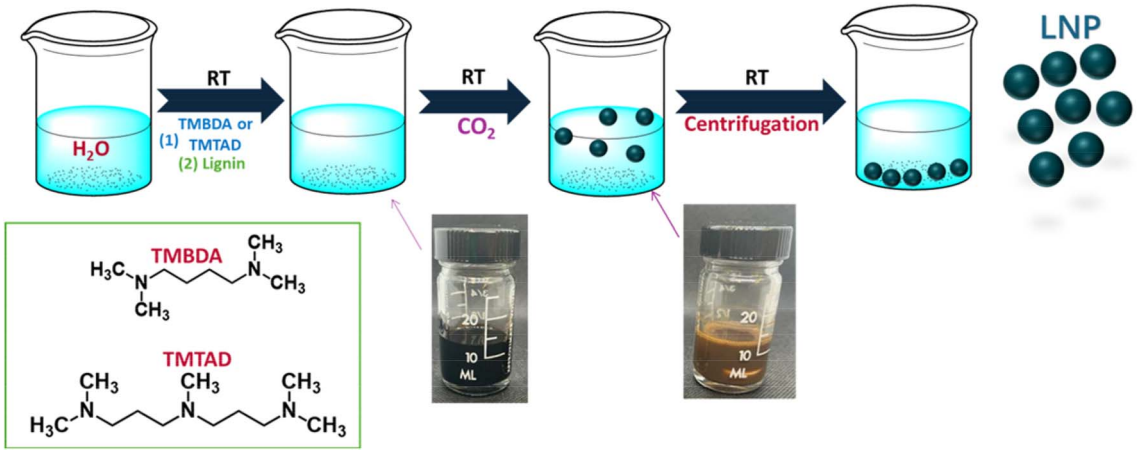

Scheme 1 Process for obtaining LNP from Kraft lignin using TMTAD or TMBDA and CO_2.

with a porous fritted glass tip, to decrease the pH and induce the formation of LNP. The entire process was carried out at room temperature. To recover the LNP, the dispersion was centrifuged at 6000 rpm for 15 minutes and washed three times with 10 mL of DI water (Scheme 1). To measure the particle size, LNP were dispersed in DI water at 10 mg mL^{-1} and then sonicated in an ice bath (Fisher Scientific) for 4 cycles of 15 s at 80% amplitude. Particle size was measured by DLS. Morphology was observed *via* TEM.

Preparation of PVA-LNP films

PVA-LNP composite films were prepared by a solvent casting process. Specific amounts of LNP (to yield 2, 4 and 8 wt% of LNP content in the films) prepared *via* the methodology presented above were added to a PVA aqueous solution (5 wt%) under agitation. After 2 h of rigorous agitation, the mixtures were cast into Petri dishes and left to dry under vacuum for 24 h at room temperature. All the films had a thickness of ~1 mm. Films were analyzed by FTIR and UV-vis.

Results and discussion

Preparation of PVA-LNP films

Kraft lignin is insoluble in water at acidic or neutral conditions, and soluble only at basic conditions. The method that we present here shares some conceptual similarity to the reported methods of pH-shifting to prepare LNP in that it utilizes a change in pH to induce precipitation.[17–19,39] Using our approach, lignin is first exposed to an aqueous basic solution of TMTAD or TMBDA (pH > 9) and the pH is then decreased by sparging CO_2 into the system, whereupon the LNP precipitate. When CO_2 is introduced in the system, it reacts with H_2O and the amine (either TMTAD or TMBDA), to produce a bicarbonate salt (eqn (1)) which not only lowers the pH but increases the ionic strength. After the amine is converted to bicarbonate salts, the excess CO_2 present in the system continues to acidify the system because carbonic acid is produced.[40–43] Once the pH drops below ~7.6, the formation of the LNP occurs by precipitation and the mixture changes to a brownish colour (Fig. 1). After centrifugation and decantation, the amine and water can be reused. Reaction 1 (eqn (1)), in which B stands for base/amine, reverses once CO_2 is removed from the system (by, for example sparging with air, nitrogen or any other nonacidic gas).[31,32]

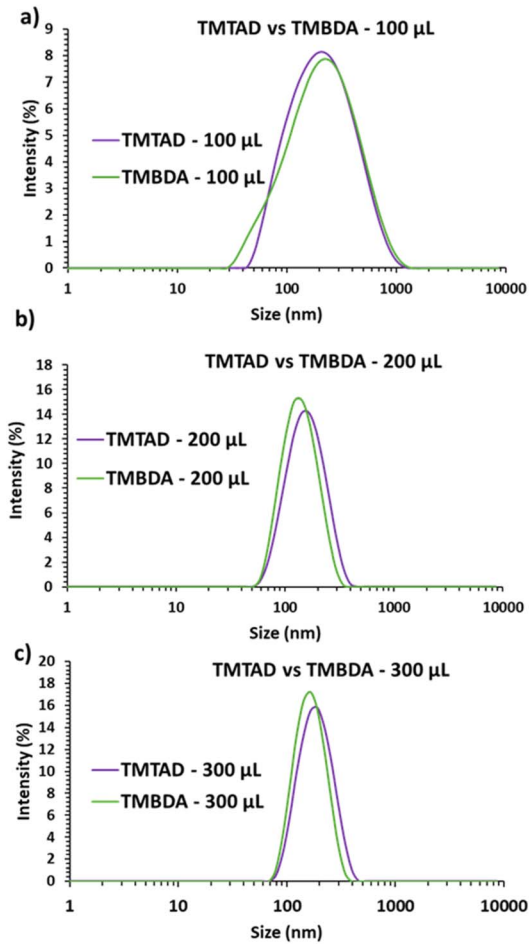

Fig. 1 Particle size distributions of LNP using TMBDA or TMTAD at 100 µL (a), 200 µL (b) and 300 µL (c).

Table 1 Amounts of amine (TMBDA and TMTAD), lignin, water, pH (before and after CO_2), particle size and PDI of the corresponding LNP

			TMBDA				TMTAD			
Water (g)	Lignin (g)	Amine (μL)	pH[a]	pH[b]	Size (nm)	PDI	pH[a]	pH[b]	Size (nm)	PDI
10	0.21	100	10.26	7.58	170	0.28	9.14	6.75	175	0.26
		200	10.76	7.52	127	0.10	9.27	6.85	144	0.11
		300	10.92	7.46	152	0.095	9.67	6.97	170	0.098

[a] Before CO_2 addition. [b] After CO_2 addition.

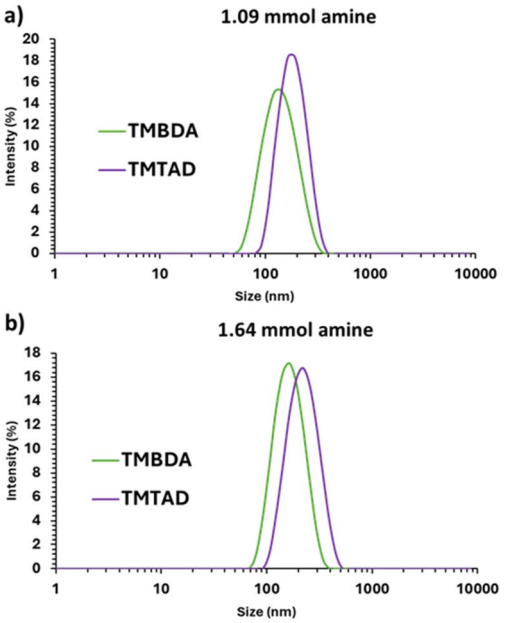

Fig. 2 Particle size distributions of LNP using TMBDA or TMTAD at 1.09 mmol (a) and 1.64 mmol (b).

$$B + H_2O \underset{-CO_2}{\overset{+CO_2}{\rightleftarrows}} [BH^+][HCO_3^-] \quad (1)$$

The reaction between TMTAD or TMBDA and CO_2 is key to the success of the LNP synthesis, and therefore we focused initially on studying the effect of the amount of TMTAD or TMBDA on the particle size and yield of LNP. The first experiments were carried out at 2 wt% lignin content. Table 1 shows the different amounts of TMTAD or TMBDA used, and the resulting mean particle size and PDI of the LNP. Fig. 2 shows the particle size distributions. Increasing the amount of amine from 100 to 200 μL decreases the particle size and narrows the distribution but upon increasing to 300 μL the particle size is slightly higher with similar PDI. When 300 μL are used, the pH is the highest among the three different concentrations, so the pH decreases to only ~7.0–7.5 upon CO_2 addition which presumably inhibits the precipitation of smaller nanoparticles.

TMBDA has a slightly higher pK_{aH} (pK_a of the amine in the protonated form) compared to TMTAD, 10.3 *vs.* 10.0,[44,45] respectively, and therefore is able to generate slightly higher pH values (see Fig. S1 and S2). Despite that difference, the two amines yield very similar particle size distributions.

The performance of the two amines was also compared on a molar basis, as opposed to the volumetric basis as discussed above. Equimolar amounts of either TMTAD or TMBDA were used (Table 2) and the particle size distribution measured (Fig. 2a and b). In this case a similar qualitative effect was observed as what was presented in Table 1; when increasing the number of mmol for both amines, the particle size increases slightly while the breadth of the distribution is similar. The effect of the amine type on the yield was also determined. TMTAD showed better performance; the yield was ~94–96% with a particle size of 144 nm (PDI = 0.11) compared with TMBDA where the yield was ~84–87% with a particle size of 149 nm (PDI = 0.13).

TEM analysis was carried out in order to observe the morphology of the LNP obtained with TMTAD (Fig. 3). TEM images showed sphere-like morphology, but the particles were not perfectly spherical. Bulk lignin and the LNP were analyzed for % C, % H and % N content using elemental analysis to determine the quantity of residual amine in the LNP. Based on the results presented in Table 3, the amounts of amine initially added the system and the final % N in the LNP, it is calculated that of the TMBDA initially fed into the system, most was

Table 2 Amounts of amine (TMBDA and TMTAD), mmol, lignin, water, particle size and PDI of the corresponding LNP

			TMBDA						TMTAD					
Water (g)	Lignin (g)	mmol amine	Amine (μL)	pH[a]	pH[b]	Size (nm)	PDI	Yield (%)	Amine (μL)	pH[a]	pH[b]	Size (nm)	PDI	Yield (%)
10	0.21	1.09	200	10.76	7.52	127	0.10	84	260	9.74	6.99	173	0.06	94
		1.64	300	10.92	7.46	152	0.095	86	400	10.07	7.06	206	0.08	95

[a] Before CO_2. [b] After CO_2.

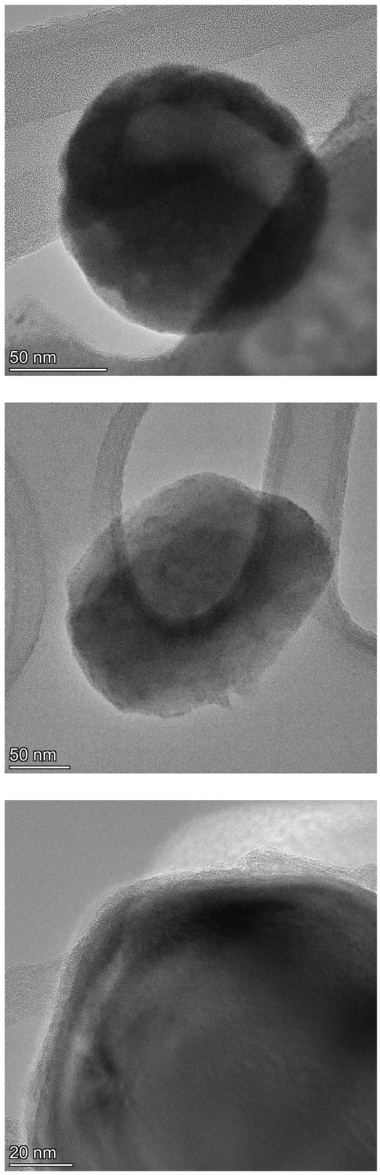

Fig. 3 TEM images of LNPs obtained with TMTAD (90 μL) and CO_2 at 2 wt%.

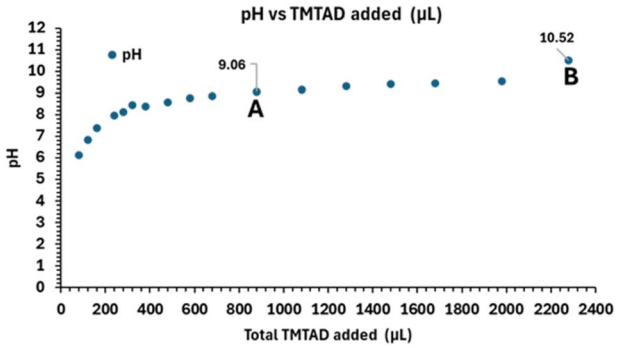

Fig. 4 pH *vs.* total TMTAD present during the process at 20 wt% lignin (2.5 g of lignin dispersed into 10 g of water). (A) Mixture becomes black, indicating complete lignin dissolution. Sample taken, sparged with CO_2, LNP obtained and purified, and particle size was measured (208 nm, PDI = 0.19). (B) Experiment stopped and mixture sparged with CO_2, LNP obtained and purified, and particle size was measured (176 nm, PDI = 0.16, yield 92%).

removed during the purification process and only about 14–15% remained in the LNP. For TMTAD only about 9–13% remained in the particles. Further work could likely lead to reduction of the residual amine levels in the LNP. TMTAD was chosen over TMBDA for further study because it is less expensive, somewhat more readily removed, and gives comparable particle size and distribution.

Initial experiments to recover the amine and potentially reuse it to prepare LNP were carried out. TMTAD or TMBDA can be deprotonated by applying nitrogen at moderately elevated temperatures (eqn (1)). Water from the washing process that contains TMTAD (in this example) was recovered and collected. Its initial pH was 7.73 but after sparging nitrogen at 45 °C, the pH increased to 9.28. This change in the pH indicates substantial but certainly not complete deprotonation of the amine. These are preliminary results, and more experiments are being carried out to demonstrate the feasibility of the recycling of the amine to synthesize LNP.

This method for LNP production would be more efficient if higher lignin loadings could be used. We therefore conducted titration studies at a higher loading (20 wt%) to determine the minimum amount of TMTAD necessary to obtain complete dissolution of the lignin. As previously noted, pH >∼ 9–10 is required to fully dissolve lignin in aqueous systems; we stopped TMTAD addition once complete dissolution was achieved, as additional TMTAD beyond what is required for dissolution results in lower yields at the precipitation step. Lignin (2.5 g) was dispersed into 10 g of water, and then TMTAD was titrated into the sample (Fig. 4). When the mixture reached pH ∼ 9.06, it became black and no agglomerates were observed, indicative of complete lignin dissolution. A portion of the solution was sparged with CO_2 to precipitate the LNP, which were then

Table 3 Elemental analysis (% C, % H, % N) of Kraft lignin and LNP

Water (g)	Lignin (g)	Amine	Amine amount (μL)	% C	% H	% N	g_{amine}/g_{LNP}	% Amine removed
10	0.21	TMBDA	200	63.29	6.78	1.93	0.11	85.87
			300	62.49	6.79	1.86	0.14	86.21
		TMTAD	200	63.41	6.79	2.11	0.11	87.39
			300	63.27	62.72	2.01	0.10	91.30
Kraft lignin				61.51	5.98	0.06	—	

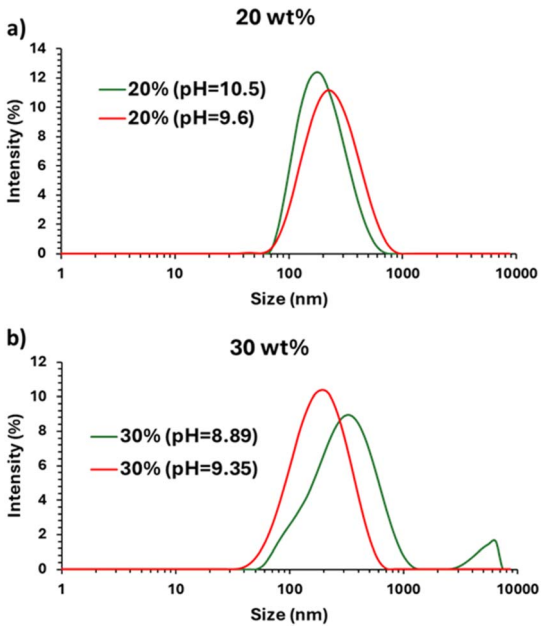

Fig. 5 Particle size distribution of LNPs prepared at different pH and lignin concentrations, 20 wt% (a) and 30 wt% (b).

purified by washing (Fig. 5a). The mean particle size was 208 nm (PDI = 0.19). In a subsequent experiment, further TMTAD was added to the remainder of the solution until the pH reached ~10.52, and LNP were again generated by CO_2 addition. The mean particle size produced with the higher pH of 10.52 was 176 nm (PDI = 0.16), slightly smaller than when the initial pH was 9.06 but significantly more amine was required when the pH was initially raised to 10.52 (2280 *vs.* 880 μL).

A similar study was carried out at 30 wt% lignin (4.28 g) dispersed into water (10 g), as seen in Fig. 6. When the system reached pH ~ 8.89, the mixture became black, a sample was taken, and the LNP were precipitated by the addition of CO_2. The average particle size was 236 nm and the distribution considerably broader (PDI = 0.36) than observed at 20 wt% lignin loading. The distribution shows a possible large particle population (beyond the detection limit of the DLS). TMTAD

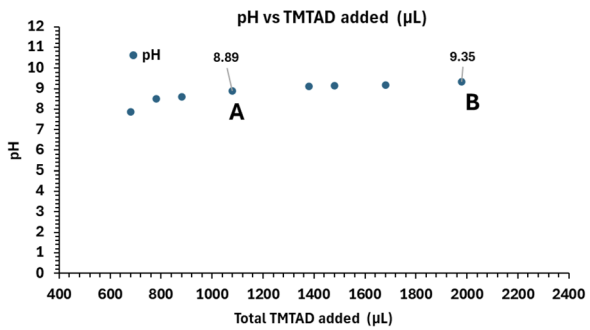

Fig. 6 pH *vs.* total TMTAD present during the process at 30 wt% lignin (4.28 g of lignin dispersed into 10 g of water). (A) Mixture becomes black. Sample taken, sparged with CO_2, LNP obtained and purified, and particle size was measured (232 nm, PDI = 0.36). (B) Experiment stopped and sparged with CO_2, LNP obtained and purified, and particle size was measured (138 nm, PDI = 0.20, yield 87%).

addition was continued until pH reached ~9.35, and LNP again generated from this pH. The particle size was 138 nm (PDI = 0.20). The distribution was slightly broader, compared to the previous experiment at 20 wt%, but was monomodal with no large particle population observed (Fig. 5b).

UV-shielding performance of PVA-LNP films

PVA-LNP films were prepared using LNP (144 nm, PDI = 0.11) prepared using TMTAD, as described in the experimental methods section. The FTIR spectra for LNP and PVA-LNP films (0, 2, 4 and 8 wt% LNP in PVA) are shown in Fig. 7. The spectra for LNP and the films show stretching vibrations of the O–H and C–H bonds at 3200–3300 and 2800–3000 cm^{-1}, respectively, characteristic of LNP and PVA. The signal at ~1650 cm^{-1} of the LNP spectra corresponds to physically absorbed water.[27] The stretching of the carbonyl group (C=O) group at 1711 cm^{-1} is attributed to unhydrolyzed PVA (PVA is obtain from the hydrolysis of poly(vinyl acetate)). The C–H stretching vibrations of LNP at 1450–1460 cm^{-1} are attributed to the aromatic rings of the phenylpropanolic monomers whereas these signals on the films can also be attributed to the C–H stretching of the PVA polymer backbone. The region of 960 to 1160 cm^{-1} in the LNP represents the C–O stretching vibrations of the lignin ether linkages and for the films can be attributed to the C–O of the C–OH bonds.

UV-vis spectroscopy was used to evaluate the UV-light shielding ability of the PVA-LNP films (Fig. 7a). Photographs of the films are shown in Fig. 7b. The control sample of pure PVA (PVA-LNP-0%) is visibly clear and colourless, exhibiting high transmittance as low as 250 nm, effectively giving no shielding against UV-light (200–400 nm). The performance of the films containing LNP is quite different. As the concentration of LNP increases, shielding of UV light improves, considering UVB (280–315 nm) and UVA (315–400 nm), reaching the maximum shielding at 8 wt% of LNP content (Table 4). In the

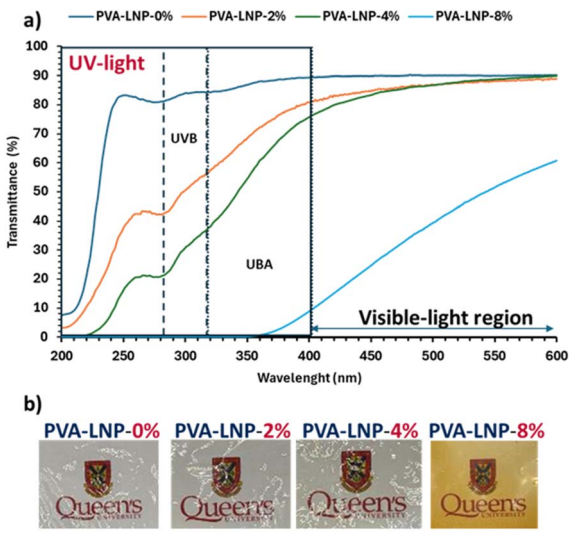

Fig. 7 (a) UV-vis spectra of PVA-LNP films (0, 2, 4 and 8 wt% LNP) (b). Photographs of the different PVA-LNP films (0, 2, 4 and 8 wt%).

Table 4 % Transmittance at 280, 315, 350 and 400 nm of the different PVA-LNP films at different LNP content (% LNP)

	% Transmittance at			
% LNP	280 nm	315 nm	350 nm	400 nm
0	81.06	84.42	86.83	89.37
2	42.28	55.38	68.53	80.92
4	21.25	36.33	54.49	75.80
8	0	0	0	9.10

case of 2 and 4% LNP loading, films reached a transmittance of 90% in the visible light region, maintaining their transparency, but in the case of 8 wt% loading, the transmittance in the visible light region was greatly decreased and the film was yellow which is aesthetically undesirable for some applications.

The study presented here in which the amines TMTAD or TMBDA are used to obtain LNP, represents a clear advantage over the existing processes to prepare LNP using strong inorganic bases such as concentrated NaOH solutions, since handling these kinds of bases require special procedures and they are corrosive. In the processes using strong bases, once the lignin is solubilized the pH needs to be reduced using an acid, forming a salt as byproduct, which precludes recovery/reuse of the NaOH.[19,46] In contrast, we have demonstrated that CO_2-switchable bases can be deprotonated using a non-acidic gas (*e.g.*, nitrogen or air) and mild temperature, and can be recycled and reused,[47,48] thereby reducing costs and at the same time reducing harm to the environment. The CO_2, in theory, could also be recovered and reused, although we have not attempted that at lab scale.

Conclusions

In this report, we present the proof of concept of a new method for producing lignin nanoparticles using two different CO_2-responsive amines in water. TMTAD and TMBDA exhibit similar performance with only small differences, with TMBDA and TMBDA producing very similar particle sizes, although the yield is slightly higher with TMTAD. Our current efforts are focused on recovering and re-using the amine to give a process involving minimal net consumption of amine. The LNP synthesized in this work were dispersed in PVA films and their performance as UV-light shields evaluated. A PVA film of 1 mm thickness, containing 4 wt% LNP, blocks ~80% of UVB light and yet is clear and almost colourless. Thus, the LNP could be used as UV-blocking filler or additive in formulations. This could represent an important application field for LNP since it has been reported that conventional chemical UV-blockers can cause chronic reproductive effects to aquatic life at low exposure levels whereas lignin is a bio-based material.[49] The process presented in this report is still a proof of concept at laboratory scale, and requires optimization (including an economic evaluation) prior to scaleup. However, a process based upon CO_2 switching of a tertiary amine is currently used at industrial scale for another application. This process could leverage the properties of lignin to enable new bio-based products or applications as a filler in polymer composites.

Conflicts of interest

There are no conflicts to declare.

Data availability

The authors confirm that the data supporting the findings of this study are available within the article.

Supplementary information (SI) is available. See DOI: https://doi.org/10.1039/d6ra01472k.

Acknowledgements

This project was supported by funds from a Mitacs Accelerate Grant.

Notes and references

1 P. Figueiredo, K. Lintinen, J. T. Hirvonen, M. A. Kostiainen and H. A. Santos, *Prog. Mater. Sci.*, 2018, **93**, 233.
2 V. K. Thakur and M. K. Thakur, *Int. J. Biol. Macromol.*, 2015, **72**, 834.
3 S. Beisl, A. Miltner and A. Friedl, *Int. J. Mol. Sci.*, 2017, **18**, 1244.
4 Q. Tang, Y. Qian, D. Yang, X. Qiu, Y. Qin and M. Zhou, *Polymers*, 2020, **12**, 2471.
5 B. Ahvazi, E. r. Cloutier, O. Wojciechowicz and T.-D. Ngo, *ACS Sustain. Chem. Eng.*, 2016, **4**, 5090.
6 W. O. Doherty, P. Mousavioun and C. M. Fellows, *Ind. Crop. Prod.*, 2011, **33**, 259.
7 P. C. Bruijnincx and B. M. Weckhuysen, *Nat. Chem.*, 2014, **6**, 1035.
8 B. M. Upton and A. M. Kasko, *Chem. Rev.*, 2016, **116**, 2275.
9 K. Koljonen, M. Österberg, M. Kleen, A. Fuhrmann and P. Stenius, *Cellulose*, 2004, **11**, 209.
10 M. Norgren and H. Edlund, *Curr. Opin. Colloid Interface Sci.*, 2014, **19**, 409.
11 B. Zhu, Y. Xu and H. Xu, *Nano Futures*, 2022, **6**, 032004.
12 A. Rangan, M. Manjula, K. Satyanarayana and R. Menon in *Biodegradable Green Composites*, S. Kalia, John Wiley & Sons, Inc, 2016, vol. 7, pp. 167–198.
13 M. H. Sipponen and L. Liu, *Advances in Lignin Chemistry: Characterization, Isolation, and Valorization*, Y. Liao and B. F. Sels, John Wiley & Sons, 2024, pp. 369–400.
14 Y. Qian, Q. Zhang, X. Qiu and S. Zhu, *Green Chem.*, 2014, **16**, 4963.
15 M. Lievonen, J. J. Valle-Delgado, M.-L. Mattinen, E.-L. Hult, K. Lintinen, M. A. Kostiainen, A. Paananen, G. R. Szilvay, H. Setälä and M. Österberg, *Green Chem.*, 2016, **18**, 1416.
16 S. Modi, M. B. Foston and P. Biswas, *ACS ES&T Eng.*, 2023, **3**, 671.
17 L. Chen, X. Zhou, Y. Shi, B. Gao, J. Wu, T. B. Kirk, J. Xu and W. Xue, *Chem. Eng. J.*, 2018, **346**, 217.

18 M. H. Sipponen, H. Lange, M. Ago and C. Crestini, *ACS Sustainable Chem. Eng.*, 2018, **6**, 9342.
19 M. Sharma, J. Marques, A. Simões, M. M. Donato, O. Cardoso and L. M. Gando-Ferreira, *Int. J. Biol. Macromol.*, 2024, **269**, 131881.
20 Y. Qian, X. Zhong, Y. Li and X. Qiu, *Ind. Crop. Prod.*, 2017, **101**, 54.
21 A. Manisekaran, P. Grysan, B. Duez, D. F. Schmidt, D. Lenoble and J.-S. Thomann, *J. Colloid Interface Sci.*, 2022, **626**, 178.
22 Q. Lu, M. Zhu, Y. Zu, W. Liu, L. Yang, Y. Zhang, X. Zhao, X. Zhang, X. Zhang and W. Li, *Food Chem.*, 2012, **135**, 63.
23 A. A. Myint, H. W. Lee, B. Seo, W.-S. Son, J. Yoon, T. J. Yoon, H. J. Park, J. Yu, J. Yoon and Y.-W. Lee, *Green Chem.*, 2016, **18**, 2129.
24 A. P. Richter, J. S. Brown, B. Bharti, A. Wang, S. Gangwal, K. Houck, E. A. Cohen Hubal, V. N. Paunov, S. D. Stoyanov and O. D. Velev, *Nat. Nanotechnol.*, 2015, **10**, 817.
25 A. K. Gupta, S. Mohanty and S. K. Nayak, *Mater. Focus*, 2014, **3**, 444.
26 W. Yang, J. M. Kenny and D. Puglia, *Ind. Crop. Prod.*, 2015, **74**, 348.
27 C. Frangville, M. Rutkevičius, A. P. Richter, O. D. Velev, S. D. Stoyanov and V. N. Paunov, *ChemPhysChem*, 2012, **13**, 4235.
28 A. P. Richter, B. Bharti, H. B. Armstrong, J. S. Brown, D. Plemmons, V. N. Paunov, S. D. Stoyanov and O. D. Velev, *Langmuir*, 2016, **32**, 6468.
29 S. Beisl, P. Loidolt, A. Miltner, M. Harasek and A. Friedl, *Molecules*, 2018, **23**, 633.
30 A. A. Myint, H. W. Lee, B. Seo, W. S. Son, J. Yoon, T. J. Yoon, H. J. Park, J. Yu, J. Yoon and Y. W. Lee, *Green Chem.*, 2016, **18**, 2129.
31 S. M. Mercer and P. G. Jessop, *ChemSusChem*, 2010, **3**, 467.
32 I. T. Cunha, H. Yang and P. G. Jessop, *Green Chem.*, 2021, **23**, 3996.
33 O. ur Rahman, S. Shi, J. Ding, D. Wang, S. Ahmad and H. Yu, *New J. Chem.*, 2018, **42**, 3415.
34 X. He, F. Luzi, X. Hao, W. Yang, L. Torre, Z. Xiao, Y. Xie and D. Puglia, *Int. J. Biol. Macromol.*, 2019, **127**, 665.
35 B. Rukmanikrishnan, S. Ramalingam, S. K. Rajasekharan, J. Lee and J. Lee, *Int. J. Biol. Macromol.*, 2020, **153**, 55.
36 Y. Li, S. Zhao, Y. Li, A. J. Ragauskas, X. Song and K. Li, *Int. J. Biol. Macromol.*, 2022, **223**, 1287.
37 A. Moreno, M. Morsali, J. Liu and M. H. Sipponen, *Green Chem.*, 2021, **23**, 3001.
38 D. Tian, J. Hu, J. Bao, R. P. Chandra, J. N. Saddler and C. Lu, *Biotechnol. Biofuels*, 2017, **10**, 1.
39 C. Frangville, M. Rutkevičius, A. P. Richter, O. D. Velev, S. D. Stoyanov and V. N. Paunov, *ChemPhysChem*, 2012, **13**, 4235.
40 A. K. Alshamrani, J. R. Vanderveen and P. G. Jessop, *Phys. Chem. Chem. Phys.*, 2016, **18**, 19276.
41 K. J. Boniface, R. R. Dykeman, A. Cormier, H.-B. Wang, S. M. Mercer, G. Liu, M. F. Cunningham and P. G. Jessop, *Green Chem.*, 2016, **18**, 208.
42 M. F. Cunningham and P. G. Jessop, *Green Mater*, 2014, **2**, 53.
43 M. F. Cunningham and P. G. Jessop, *Macromolecules*, 2019, **52**, 6801.
44 D. E. Leyden and J. McCall Jr, *J. Phys. Chem.*, 1971, **75**, 2400.
45 R. Rometsch, A. Marxer and K. Miescher, *Helv. Chim. Acta*, 1951, **34**, 1611–1618.
46 C. Frangville, M. Rutkevičius, A. P. Richter, O. D. Velev, S. D. Stoyanov and V. N. Paunov, *ChemPhysChem*, 2012, **13**, 4235–4243.
47 M. Sanger, D. Barker and P. G. Jessop, *Phys. Chem. Chem. Phys.*, 2024, **26**, 11406–11413.
48 X. Su, P. G. Jessop and M. F. Cunningham, *Macromolecules*, 2018, **51**, 8156–8164.
49 P. G. Jessop, F. Ahmadpour, M. A. Buczynski, T. J. Burns, N. B. Green II, R. Korwin, D. Long, S. K. Massad, J. B. Manley, N. Omidbakhsh, R. Pearl, S. Pereira, R. A. Predale, P. G. Sliva, H. VanderBilt, S. Weller and M. H. Wolf, *Green Chem.*, 2015, **17**, 2664–2678.